

Reliability study of pellet ELM pace making

G. Kocsis^a, P.T.Lang^b, G. Cseh^a, M. Dunne^b, L. Horváth^d, V. Mertens^b, H. Meyer^c,
 B. Ploeckl^b, G. I. Pokol^d, P. Zs. Pölöskei^d, B. Sieglin^b, T. Szepesi^a, E. Viezzer^b,
 EUROfusion MST1 Team¹ and ASDEX Upgrade Team

^a*Wigner RCP RMI, Konkoly Thege u. 29-33, H-1121 Budapest, Hungary*

^b*MPI für Plasmaphysik, Boltzmannstr. 2, 85748 Garching, Germany*

^c*CCFE, Culham Science Centre, Abingdon, Oxon, OX14 3DB, UK*

^d*BME NTI, Budapest, Hungary*

Injection of cryogenic solid hydrogen isotope pellets turned out to become a potentially powerful tool for ELM pace making in large-scale toroidal machines like ITER. According to scenario requirements, pacing is needed for ELM mitigation and/or to prevent impurity accumulation [1]. Since its discovery at ASDEX Upgrade (AUG) [2], the pellet ELM pacing technique has been confirmed on other tokamaks such as DIII-D [3] and JET [4]. An increase of the spontaneous ELM frequency by a factor of up to 12 was demonstrated at DIII-D, providing the proof that pellet ELM pacing is a reliable control tool[3]. Experiments and simulations showed that ELMs can be initiated by the toroidally localized high pressure edge regions formed by the localized particle deposition by the ablating pellet. However, most of these results had been obtained in devices where at least parts of the plasma facing components had carbon surfaces. In modern, more reactor relevant all-metal wall machines – due to the change in operational conditions imposed by the metallic wall - significant changes of the pedestal conditions and the ELM dynamics were observed. This implies that the reliability of pellet ELM pace making technique should be reconsidered as well.

Accordingly, the EUROfusion MST1 work package and the last campaigns of AUG put special emphasis to investigate the reliability of pellet ELM triggering and to understand the underlying physics of pellet ELM pace making. First experiments on all-metal wall AUG revealed that - in spite of similar pellet caused perturbations - the pellet ELM triggering potential was reduced in certain plasma scenarios. In general it was found that the probability of a pellet triggering an ELM is dependent on the time elapsed since the previous ELM and even “lag times” were observed where this probability drops to zero. It was also revealed that the pellet ELM triggering potential is independent of the pellet parameters (mass, speed, injection frequency), that is, of the pellet imposed perturbation - at least in the technically accessible parameter range. Conversely the triggering potential was clearly dependent on the scenario of the target plasma and it seemed to be that Nitrogen seeding helps to recover some of the pellet triggering potential.

This phenomenon was investigated in detail and the results are presented in this contribution. As target plasma an edge optimised configuration was used with moderate heating resulting in a long stable plateau phase with 300-400kJ plasma energy content and type-I ELMs with an energy drop up to 25kJ. To avoid global plasma perturbation small pellets were injected

¹ See <http://www.euro-fusionscipub.org/mst1>

into this plateau phase with low frequency (4Hz). In order to provide accurate T_e , T_i and n_e profiles in the pedestal region for stability analysis a reference phase was also included into the scenarios before the start of the pellet injection sequence.

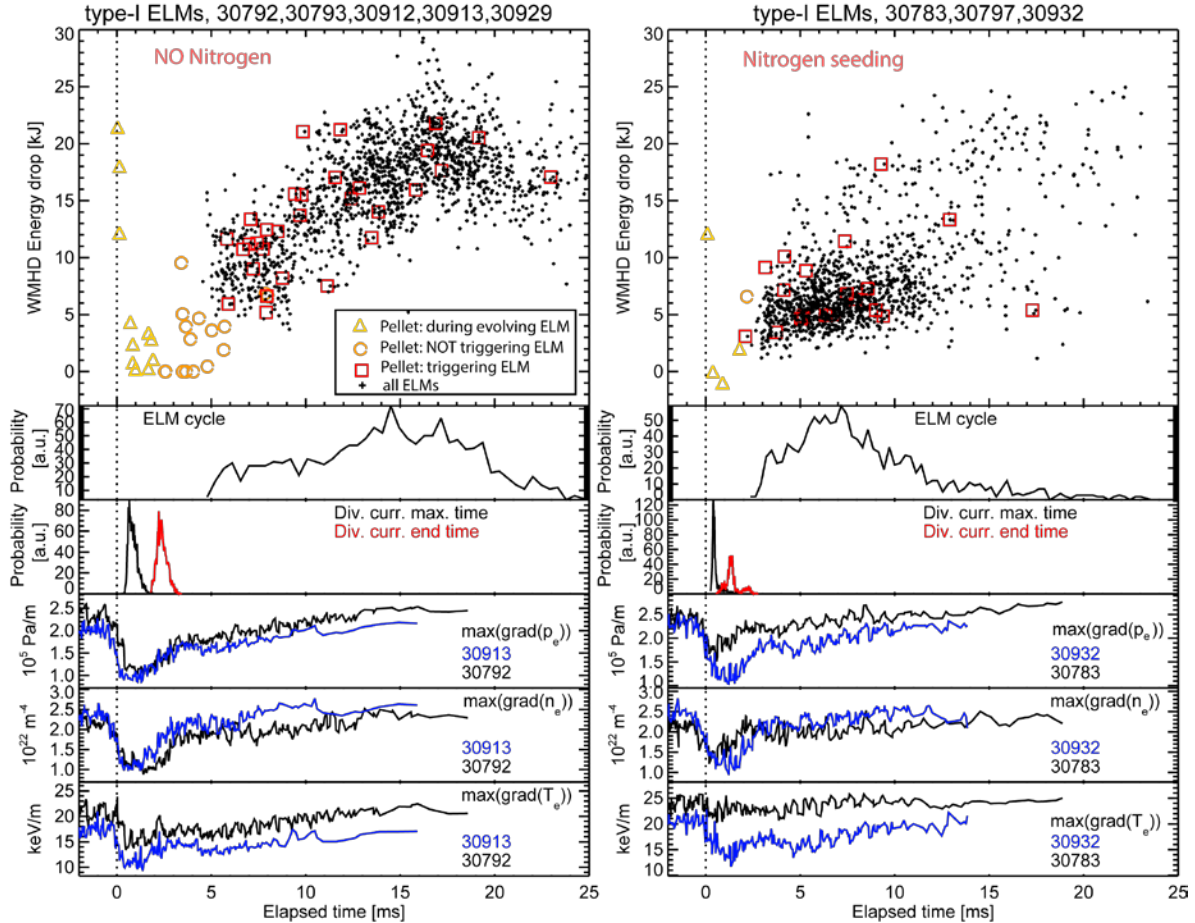


Fig. 1. The ELM provoked plasma energy drop as a function of the time elapsed after the previous ELM both for spontaneous and pellet triggered ELMs. The right column shows the Nitrogen seeded case (puff rate is about $2.5 \times 10^{21} \text{ s}^{-1}$), while the left column is for similar discharges without Nitrogen puffing. The evolution of the pedestal gradients and statistics about the ELM dynamics (cycle, crash dynamics characterised by the divertor current measurements) are also plotted for both cases.

With this low pellet injection rate the ELM appearance is uncorrelated to the pellets' arrival therefore every pellet hits the plasma at an arbitrary time point in the spontaneous ELM cycle. To collect enough 'pellet events' that is to map the whole ELM cycle the discharge was repeated several times and the experiment was also repeated with Nitrogen seeding applied. The results are summarised in Fig.1 together with the evolution of the pedestal gradients and statistics about the ELM dynamics. Generally it can be observed that pellets can trigger ELMs at elapsed times at which spontaneous ELMs also occur. For the scenario without Nitrogen puffing a lag time of about 5ms (one third of the ELM cycle) is found. Nitrogen seeding (Fig.1., right column) shortens the lag time, but also modifies the target plasma resulting in a better confinement, smaller ELMs, shorter ELM cycle, ELM crash and recovery time. It seems to be that for both seeded and unseeded cases pellets can trigger ELMs after the fast recovery phase of the pedestal (see the evolution of the pedestal

gradients). To compensate the confinement improvement caused by the Nitrogen seeding more heating power was also added to the non-seeded scenario (reaching the same plasma energy content as for the seeded case) but this neither changes the ELM cycle and dynamics nor shortens the lag time.

Pellet tracking and the investigation of the ELM onset detected by magnetic pick-up coils revealed that if pellets trigger ELMs the triggering happens shortly after the pellets crossing the separatrix. The time delay of the magnetic ELM onset after the pellet separatrix crossing time lies typically between 0 and 150 μ s and decreases with increasing elapsed time (similarly to the carbon wall cases). No significant difference was found between the non-seeded and seeded scenario which implies that the pellet imposed perturbation needed to trigger an ELM is independent of the seeding.

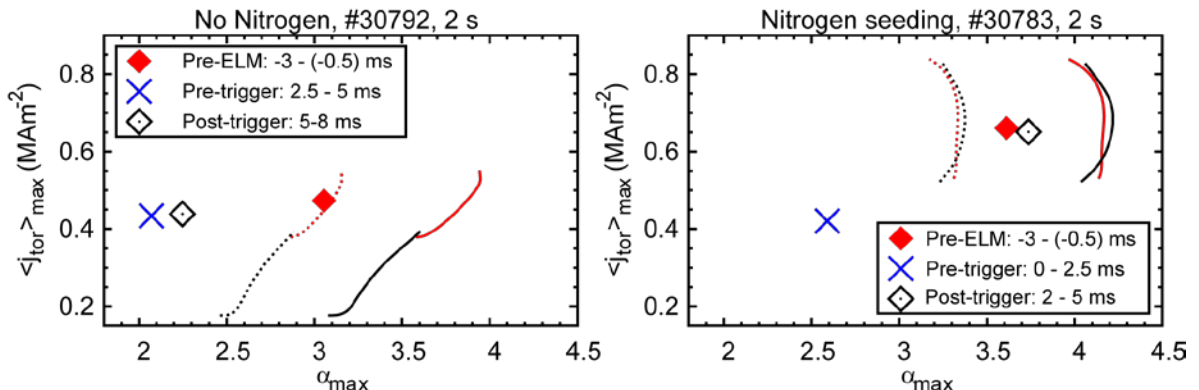


Fig. 2. Stability shown as a function of the stability parameters, the pressure gradient and the current density. α_{\max} is the maximum normalized edge pressure gradient and the maximum toroidal edge current density is flux surface averaged. The operational point and the stability boundary are calculated for three phases: **just before the ELM (pre-ELM)**, **during the lag time (pre-trigger)** and **where already pellets can trigger (post-trigger)**. To indicate the accuracy of the calculation the shifted stability boundaries to 80% of the pressure gradient are also over plotted (dotted lines).

The target plasma scenarios were modelled by axial symmetric linear peeling-ballooning (LPB) model which gives indication about the plasma stability. Note that since this analysis assumes toroidal symmetry while the perturbation has a strong 3D character obviously the analysis with full 3D treatment (e.g. by JOREK) would be useful in the future. In the LPB model the kinetic profiles, data from magnetic field and flux difference measurements were used (CLISTE Grad–Shafranov) to calculate a self-consistent plasma equilibrium and full current density profiles and the refined equilibrium was used for stability calculation (MISHKA-fast code)[6]. The results are summarised on Fig.2. both for reference and Nitrogen seeded discharges for three relevant time windows. Since pellets can trigger ELMs at elapsed times at which spontaneous ELMs also occur, we expect that in these cases the plasma is close to the stability boundary. This is more or less confirmed by the LPB calculations. In the reference case, both the pre- and post-trigger cases are far from the stability boundary, indicating that a natural ELM is unlikely to occur at both of these time points (though they can be observed in the post-trigger phase). In the nitrogen seeded case, the post-trigger case is close to the stability boundary, which is likely to be due to the shorter ELM cycle in this case; a separation of the probabilities of natural and triggered ELMs is

only possible in the reference discharge (see also Fig.1 for the probability distribution over the ELM cycle).

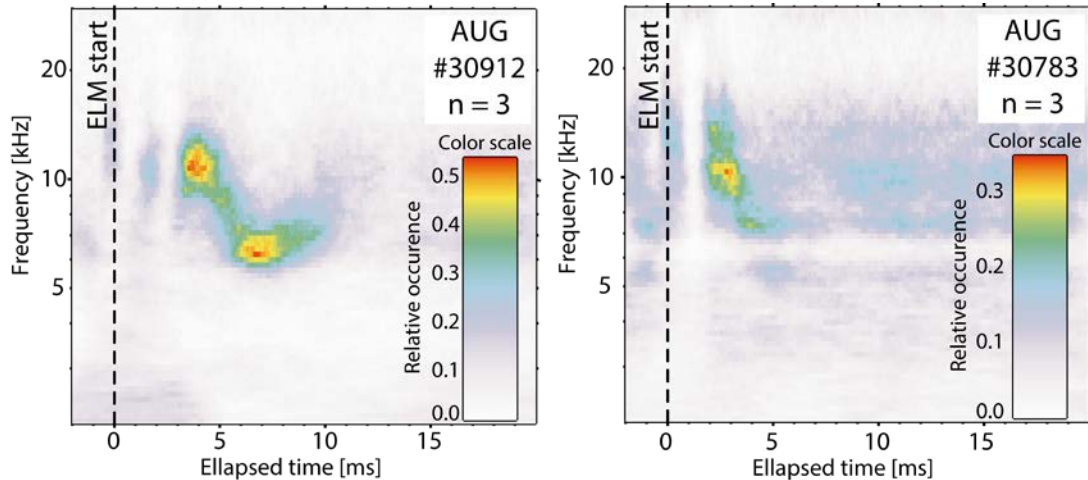


Fig. 3. Time-frequency mode number analysis for toroidal mode number 3 for the non-seeded (left) and seeded scenario (right).

In order to reveal differences for the different stability phases a statistical time-frequency mode number analysis was performed for 283 and 493 ELMs in non-seeded and seeded shots, respectively. The first step of this process was a continuous wavelet decomposition by order 24 Morlet wavelets in the [-2,20 ms] time interval with respect to the ELM start, for the toroidal magnetic probe array. Using the cross-phases of the transforms the most probable mode numbers were determined at each time-frequency point. Fig.3. shows the probability of the occurrence of the $n=3$ toroidal mode at each time-frequency point aggregated from all ELMs. This mode is the strongest component of the washboard-like modes appearing at equidistant frequencies increasing for increasing mode numbers in the range of $n=3-9$, propagating in the electron diamagnetic direction. Just after the ELM the washboard-like modes appear at an elevated frequency (10-11kHz), and their frequency gradually decreases to their pre-ELM frequency (6-7kHz) in the post-ELM recovery phase. The characteristic time of this frequency decrease corresponds to the lag-time after the ELMs. This indicates that the washboard mode frequency might be a good indicator for the edge plasma returning into a state susceptible to ELMs.

This work has been carried out within the framework of the EUROfusion Consortium and has received funding from the Euratom research and training programme 2014-2018 under grant agreement No 633053. The views and opinions expressed herein do not necessarily reflect those of the European Commission.

References

- [1] Loarte A. *et al* 2014 *Nucl. Fusion* **54** 033007
- [2] Lang P.T. *et al* 2004 *Nucl. Fusion* **44** 665
- [3] Baylor L.R. *et al* 2013 *Phys. Rev. Lett.* **110** 245001
- [4] Lang P.T. *et al* 2011 *Nucl. Fusion* **51** 033010
- [5] Lang P.T. *et al* 2014 *Nucl. Fusion* **54** 033009
- [6] Konz C. *et al* 2009 36th EPS Conference on Plasma Phys., *ECA* **33E** P-1.152